NAVAL POSTGRADUATE SCHOOL

MONTEREY, CALIFORNIA

THESIS

DETECTION OF FREQUENCY-HOPPED SIGNALS EMBEDDED IN INTERFERENCE WAVEFORMS

by

Christopher Brown

June 2005

Thesis Advisor:	R. Clark Robertson
Second Reader:	Frank Kragh

THIS PAGE INTENTIONALLY LEFT BLANK

REPORT DOCUMENTATION PAGE	*Form Approved OMB No. 0704-0188*

1. AGENCY USE ONLY *(Leave blank)*	**2. REPORT DATE** June 2005	**3. REPORT TYPE AND DATES COVERED** Master's Thesis

4. TITLE AND SUBTITLE: Title (Mix case letters)
Detection Of Frequency-Hopped Signals Embedded In Interference Waveforms

5. FUNDING NUMBERS

6. AUTHOR(S)

7. PERFORMING ORGANIZATION NAME(S) AND ADDRESS(ES)
Naval Postgraduate School
Monterey, CA 93943-5000

8. PERFORMING ORGANIZATION REPORT NUMBER

9. SPONSORING /MONITORING AGENCY NAME(S) AND ADDRESS(ES)
N/A

10. SPONSORING/MONITORING AGENCY REPORT NUMBER

11. SUPPLEMENTARY NOTES The views expressed in this thesis are those of the author and do not reflect the official policy or position of the Department of Defense or the U.S. Government.

12a. DISTRIBUTION / AVAILABILITY STATEMENT
Approved for public release; distribution is unlimited.

12b. DISTRIBUTION CODE

13. ABSTRACT (maximum 200 words)

Many military communications systems utilize frequency-hopped spread spectrum waveforms to protect against jamming and enemy detection. These waveforms may be subjected not only to intentional jamming but may also be unintentionally jammed by other communications signals. While some systems can overcome in-band interference with more signal power, covert systems may be limited to small amounts of transmitted power. The objective of this thesis was to investigate a method for resolving a frequency-hopped signal embedded in interference waveforms.

With exponential averaging in the frequency domain, the spectra of the interfering signals can be estimated as long as they are present over a period longer than that of the frequency-hopped signal. Certain FFT sizes and weights are more beneficial to achieving this estimate than others. The interference estimate can be used to extract the desired frequency-hopped signal through spectral division of the received signal with the estimate. This technique is designated as noise-normalization. Simulations in MATLAB demonstrate the use of the technique and show how the desired signal can be resolved.

14. SUBJECT TERMS
Noise-normalization, frequency-hopped, interference estimate, exponential average

15. NUMBER OF PAGES
57

16. PRICE CODE

17. SECURITY CLASSIFICATION OF REPORT	**18. SECURITY CLASSIFICATION OF THIS PAGE**	**19. SECURITY CLASSIFICATION OF ABSTRACT**	**20. LIMITATION OF ABSTRACT**
Unclassified	Unclassified	Unclassified	UL

NSN 7540-01-280-5500 Standard Form 298 (Rev. 2-89)
Prescribed by ANSI Std. 239-18

THIS PAGE INTENTIONALLY LEFT BLANK

Approved for public release; distribution is unlimited

DETECTION OF FREQUENCY-HOPPED SIGNALS EMBEDDED IN INTERFERENCE WAVEFORMS

Christopher K. Brown
Ensign, United States Naval Reserve
B.S., United States Naval Academy, 2004

Submitted in partial fulfillment of the
requirements for the degree of

MASTER OF SCIENCE IN ELECTRICAL ENGINEERING

from the

NAVAL POSTGRADUATE SCHOOL
June 2005

Author: Christopher Brown

Approved by: R. Clark Robertson
Thesis Advisor

Frank Kragh
Second Reader

John P. Powers
Chairman, Department of Electrical and Computer Engineering

THIS PAGE INTENTIONALLY LEFT BLANK

ABSTRACT

Many military communications systems utilize frequency-hopped spread spectrum waveforms to protect against jamming and enemy detection. These waveforms may be subjected not only to intentional jamming but may also be unintentionally jammed by other communications signals. While some systems can overcome in-band interference with more signal power, covert systems may be limited to small amounts of transmitted power. The objective of this thesis was to investigate a method for resolving a frequency-hopped signal embedded in interference waveforms.

With exponential averaging in the frequency domain, the spectra of the interfering signals can be estimated as long as they are present over a period longer than that of the frequency-hopped signal. Certain FFT sizes and weights are more beneficial to achieving this estimate than others. The interference estimate can be used to extract the desired frequency-hopped signal through spectral division of the received signal with the estimate. This technique is designated as noise-normalization. Simulations in MATLAB demonstrate the use of the technique and show how the desired signal can be resolved.

THIS PAGE INTENTIONALLY LEFT BLANK

TABLE OF CONTENTS

THIS PAGE INTENTIONALLY LEFT BLANK

LIST OF FIGURES

THIS PAGE INTENTIONALLY LEFT BLANK

LIST OF TABLES

THIS PAGE INTENTIONALLY LEFT BLANK

ACKNOWLEDGMENTS

I would like to thank Prof. Clark Robertson for his guidance, patience, and commitment to this thesis and my education. I would also like to extend a thank you to Prof. Frank Kragh for his insight on this paper and all the knowledge I have gained from his classes. Many thanks to Dr. Kyle Kowalske for the tremendous amount of time he devoted to helping me create a successful project as well. Finally, thanks to my parents and my best friend, Nicole Diane, for their 24-hour support and encouragement.

THIS PAGE INTENTIONALLY LEFT BLANK

EXECUTIVE SUMMARY

This thesis investigated recovery techniques for frequency-hopped spread spectrum signals embedded in interference waveforms. Many military communications systems utilize frequency-hopped spread spectrum techniques to protect against jamming and enemy detection. These systems operate in environments that may contain other communications signals and, as a result, may be subjected to interfering waveforms. While some systems can overcome in-band interference with more signal power, covert systems may be limited to small amounts of transmitted power. The objective of this thesis was to investigate a method for resolving a frequency-hopped signal amongst interference waveforms that might be operating in the same band.

The spectra of the interfering signals can be estimated with an exponential averaging algorithm in the frequency domain. Several N-sample windows of the received signal are transformed to the frequency domain by taking the fast Fourier transform (FFT). These windows of the received signal are averaged to create an N-point frequency domain representation of the interference waveforms. The estimate is formed under the assumption that the interference waveforms are constant over multiple hops. As a result, an individual frequency hop present in an FFT window will not be present in the final average of all the FFTs, leaving just the interference waveforms.

Certain FFT window sizes and weight factors are more beneficial to achieving this estimate than others. As the FFT window size increases, the number of FFTs used to create the estimate decreases. Too large of an FFT window causes the estimate to be formed from a small number of windows, and thus the frequency-hopped signal is not averaged out. Small FFT windows cause resolution problems though, and do not accurately represent the overall shape of frequency spikes and spectral lobes. A balance must be found in choosing the FFT window size. Moreover, the weight factor affects how much influence an individual window has on the estimate. A large weight value places more emphasis on the most recent frequency hop, while a smaller weight accentuates the first frequency hop in the sequence. The goal is to find a weight that allows each frequency hop to be reduced to an acceptable level. A good weight factor forms an estimate

that is an accurate representation of the interference waveforms, with few frequency hops remaining in the spectrum.

The estimate can be used to extract the desired frequency hops through spectral division of the received signal with the estimate. This technique is known as noise-normalization. Simulations in MATLAB demonstrate the use of the technique and show how the frequency-hopped spectra and desired signal can be resolved. A frame-by-frame division of the received signal by the estimate reveals frequency hops that are eclipsed by the spectral lobe. Given enough frames to create the estimate, a receiver is able to re-cover all but the last two hops that occur over a finite period. This technique also proves to be superior when compared with spectral subtraction. Specific FFT window sizes and weight factors lead to clearer normalized spectra and recover more frequency hops than other combinations of FFT size and weight factor. The weight factor that provides the best estimate is not necessarily the best weight for resolving the frequency-hopped signal. Bit error rate simulations of the normalization technique reveal that the noise-normalization technique achieves the same bit error rate as a 50-dB reduction in noise power.

The technique described in this thesis, though implemented only in simulation, forms an accurate estimate of interference waveforms and successfully detects frequency hops eclipsed by other signals in the band.

I. INTRODUCTION

A. BACKGROUND

Within military communications, frequency-hopped systems play a major role. These systems use changing carrier frequencies so that the signal is difficult to intercept. Frequency-hopped signals operate within a band, and each adjacent carrier is separated by some bandwidth, Δf. Given that in some areas the electromagnetic spectrum is not strictly regulated, it is possible for frequency-hopped radio links to operate amidst other signals. In the case of covert transmission, simply increasing transmission power to overcome interference that happens to be jamming the receiver is not always an option. A receiver that has a sense of the environment it is operating in should be able to adjust for the interference and recover the desired signal.

Previous work in [1]-[4] has yielded several different methods for frequency-hopped signal detection. These methods all assume that the frequency-hopped signal is being received in additive white Gaussian noise and thus has a standard mathematical estimate. From [5], it is known that the power spectral density of such noise is constant across all frequencies. The effect of real communications signals such as phase-shift keyed (PSK), minimum-shift keyed (MSK), and quadrature amplitude modulated (QAM) signals that might act as interference are more difficult to model. These signals' spectra contain spectral spikes, lobes, and nulls that cannot be approximated as additive white Gaussian noise (AWGN). This thesis investigates the detection of a frequency-hopped waveform embedded in an interference waveform consisting of a combination of a PSK signal and a number of continuous wave (CW) signals.

B. OBJECTIVES

The focus of this thesis was two-fold. The first objective was to develop a method to estimate the interference environment. The receiver must be able to use this estimate for further signal processing. With an N-point window, many small fast Fourier transforms (FFT) of the received signal can be averaged to form an estimate of the interference power spectral density. The parameters surrounding this method, including the size of the FFT window and the configuration of the averaging algorithm, are the key components in deriving the interference estimate.

The second goal was to explore methods to resolve the frequency-hopped waveform using the interference estimate. The goal was not to amplify the desired signal but to reduce the noise power level, thus increasing the signal-to-noise ratio. Detection of the frequency-hopped waveform was the end goal but was done while keeping in mind that the signal contains modulated data that eventually must be recovered. Spectral subtraction and noise-normalization were studied. Although noise-normalization has been analyzed from a theoretical standpoint, to the best of the author's knowledge, this is the first time noise-normalization has been implemented.

C. ORGANIZATION OF THESIS

This thesis consists of four parts. Background information on the signals used and the MATLAB program utilized for simulating the signal processing are described in Chapter II. Chapter III presents a description of the investigation into developing a technique for estimating the interference in the channel. Chapter IV contains a description of frequency hop recovery techniques. Chapter V contains a bit error rate simulation for a transmitted signal with the recovery technique performed on the channel. The final chapter, Chapter VI, contains conclusions and recommendations for further research.

II. SIMULATION SIGNALS

The signals used in detection simulations are described in this chapter. In order to test the various aspects of forming an interference estimate and recovering a frequency-hopped signal, discrete signal files were used within MATLAB simulations. The MATLAB program can import various types of discrete signal files into an array, including files denoted as signals with a .sig extention, which were used for this thesis. Mathematical computations, loops, if/else statements, fast Fourier transforms, and bit error rate calculations are some of the unique capabilities that the MATLAB program provided for creating various simulations. All plots shown in this paper were created using arrays in MATLAB.

The signals used for the simulation were each sampled at 50 MHz and contain 1,032,192 points of data. Three files were imported into MATLAB but were manipulated in the program to create several different signals for the simulation. Two signals were used to create an interference signal that operates in the same band as a transmitted signal. The terms "transmitted signal" and "desired signal" refer to the same frequency-hopped signal and are used interchangeably throughout this thesis.

A. DESIRED FREQUENCY-HOPPED SIGNAL

The desired signal is a frequency-hopped, minimum-shift keyed (FH/MSK) signal. An FFT of the signal is shown in Figure 1 to illustrate the frequency-domain representation of the signal. The shape of the power spectral density function is approximated by the squared magnitude of the FFT. To simplify the algorithm, the magnitude of the FFT is used to represent frequency-domain signals in this thesis. The signal hops over 5.8 MHz of spectrum, from 6.9 MHz to 12.7 MHz. Table 1 shows the approximate frequency and order of each of the seven frequency hops in the signal.

Approximate Carrier Frequency of Hop	Hop Number
6.9 MHz	5
9.58 MHz	7
9.8 MHz	4
10 MHz	1
11.65 MHz	3
12.07 MHz	6
12.7 MHz	2

Table 1. Frequencies and sequence order of hops in FH/MSK signal.

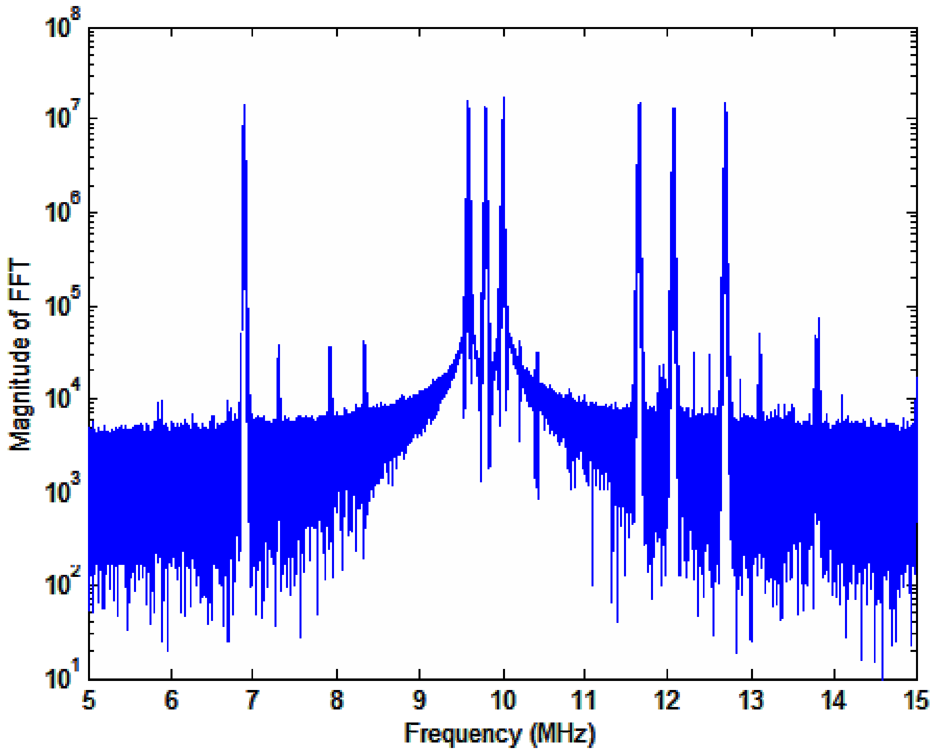

Figure 1. Fourier transform of FH/MSK transmitted signal without interference.

B. INTERFERENCE WAVEFORMS

The interference signal is a composite waveform consisting of two separate signals. The first file contains a continuous wave (CW) signal that has defined spectral components at 21 frequencies in the operating bandwidth of the frequency-hopped signal. This signal produces many spectral spikes, which closely resemble a frequency-hopped signal in the frequency domain. A plot of the magnitude of an FFT of the CW signal is shown in Figure 2. The second signal is a binary-shift keyed signal (BPSK) with a carrier frequency of 10 MHz. Figure 3 contains a plot of the power spectral density of the BPSK signal. Summing the signals together in the time domain created the total interference signal. A plot of the power spectral density of the total interference signal is shown in Figure 4.

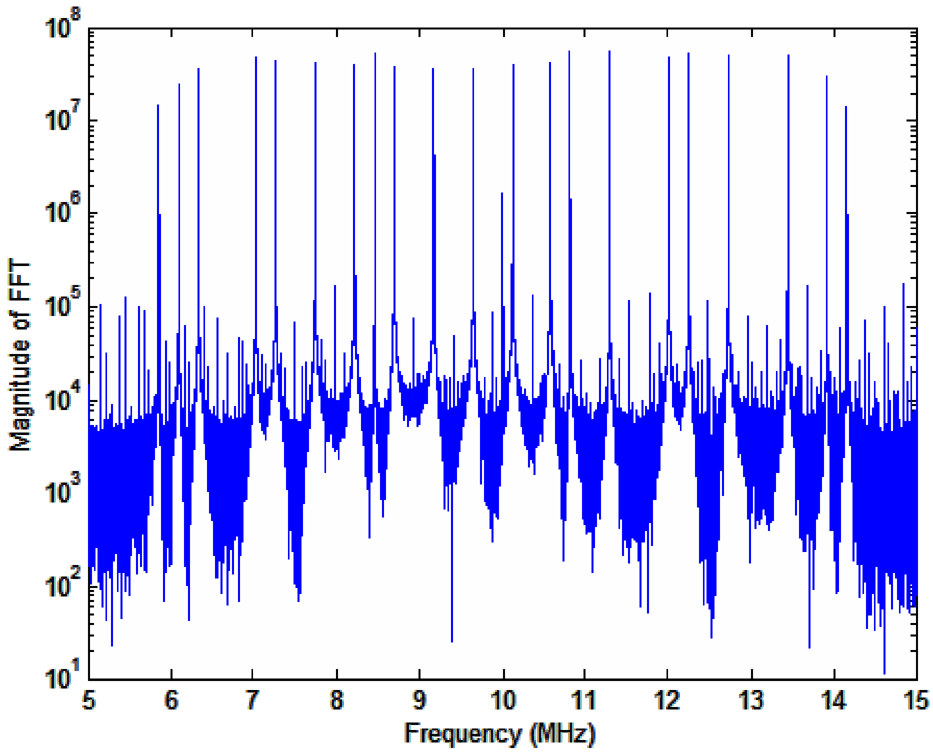

Figure 2. Fourier transform of continuous wave signal.

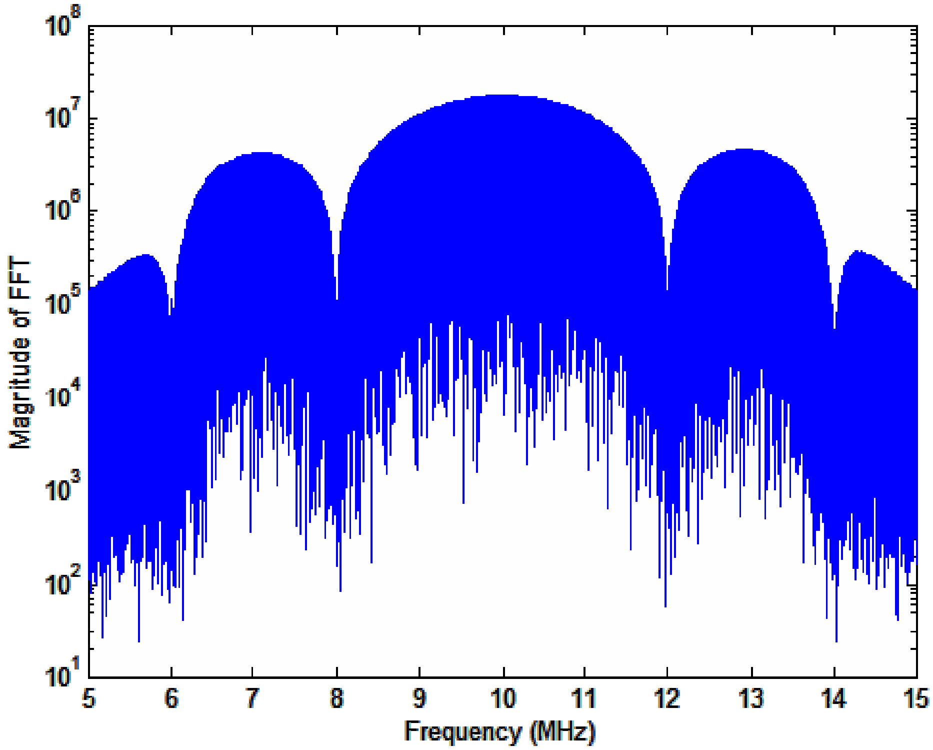

Figure 3. Fourier transform of BPSK signal.

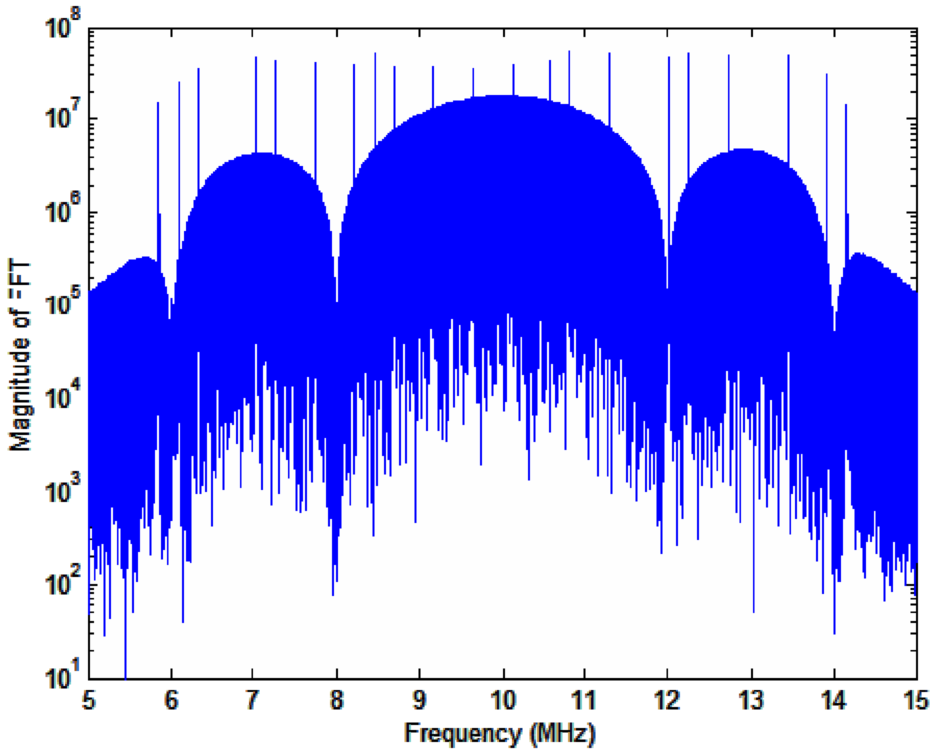

Figure 4. Fourier transform of total interference signal.

When all three signals are transmitted over the same time period, the spectrum becomes crowded and the frequency hops cannot be resolved directly. As shown in Figure 5, the frequency hops are buried amongst the BPSK interference or are otherwise difficult to distinguish from the CW signal. From Figure 5 it is evident that a filter-based detection method, like those described in [1] and [2] and shown in Figure 6, would be overwhelmed by the interference in the band. Each filter is meant to detect energy at a specific frequency, but interference signals that span the entire bandwidth of the desired signal and have a large amount of energy will cause each branch of the detector to indicate a frequency hop present at that frequency.

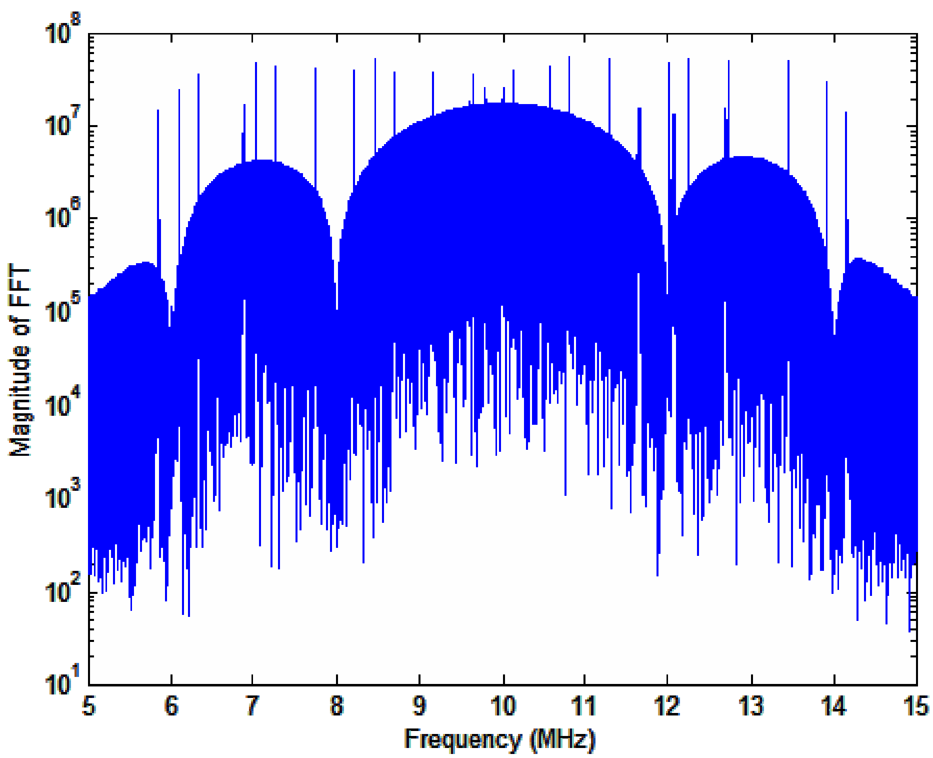

Figure 5. Frequency domain plot of total received signal.

This is a significant problem because the frequency hops are essentially being jammed by other modulated waveforms without flat power spectral densities. From [5], additive white Gaussian noise is assumed to have a flat power density across all frequencies in the band. Gaussian noise that is uniform across all frequencies in the band is easy to estimate mathematically for any frequency hop in the spectrum. The spectral variations of a communications signal such as the interference waveform mentioned in this thesis cannot be approximated as Gaussian noise.

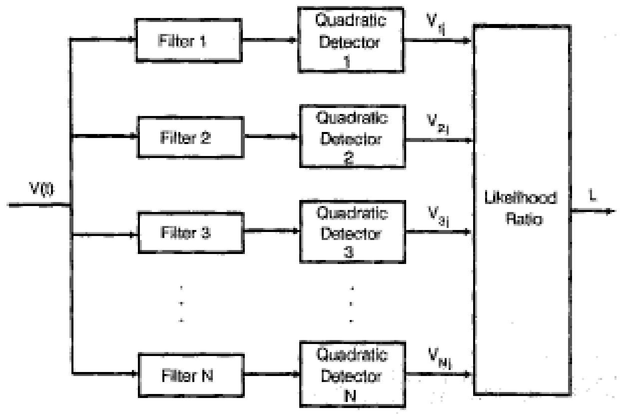

Figure 6. Channelized receiver followed by likelihood-ratio test (From Ref. 1.).

The signals used in the simulations were described in this chapter. From an examination of past works, to the best of the author's knowledge this is the first time that frequency-hopped signal detection has been studied in an environment containing non-Gaussian noise. A FH/MSK signal is the desired transmitted signal, but at the receiver the frequency-hopped signal is eclipsed by interfering BPSK and CW waveforms. A composite of the BPSK, CW, and FH/MSK signals is treated as the total received signal. In the next chapter, the use of the exponential averaging algorithm to form an estimate of the interference signals is described.

III. INTERFERENCE ESTIMATION

In this chapter efforts to estimate the interference present in the operating band are discussed. An exponential average of FFT windows was used to create an approximate frequency-domain representation of the interference signal. The parameters of the exponential average, such as weight factor, FFT window size, and the number of windows in the average, are discussed.

A. EXPONENTIAL AVERAGE

The term interference estimation refers to a frequency-domain representation of the interference signal. In order to recover the frequency-hopped signal embedded in the interference signal, an acceptable estimate of the composite BPSK and CW signal is required. As a first step, the components of the frequency-hopped signal must be removed from the total received signal spectrum. Using an exponential average of FFT windows, we can obtain an approximate picture of the interference spectrum. This algorithm is useful for averaging a discrete signal that has an unknown length.

The interference estimate is created by exponentially averaging many small FFTs over time. The received signal, composed of the FH/MSK signal, as well as the BPSK and CW interference waveforms, was broken into *N*-point windows. The FFT of each window was computed and the magnitude of the FFT was taken. (When an FFT window is referenced in this thesis it can be assumed that it is the magnitude of a fast Fourier transform being described.) The FFT windows were used to form an estimate according to an exponential average. If the number of frames was known before averaging the windows, it would be simple to apply an equal-weight average to each window of 1/*L*, where *L* is the number of windows used to form an estimate of the interference. The length of the signal is not known, however, and thus an exponential average is used to form the interference estimate. The averaging algorithm is represented mathematically by

$$X[i] = (1-R)\cdot X[i-1] + R\cdot C[i] \tag{1}$$

where $X[i]$ is the *i*-th averaged window in the signal known as the reference frame, *R* is a weight factor between 0 and 1, $C[i]$ is an FFT of the current window in the signal, $i = 1, 2, \ldots, L$, and $L = 1,032,192/N$. The reference is multiplied by a factor of $1-R$ and added to the current frame, which is weighted by *R*. The sum then becomes the new reference frame. From (1), it can be shown that three important variables affect the final estimate: the FFT window size, *N*; the number of FFTs used to create the estimate, *L*; and the weight factor, *R*.

B. FFT SIZE

The size of the FFT affects not only the number of frames used in the estimate but also the resolution of the estimate. Since the final estimate will be the same size as the windows used to form the estimate, choosing the correct *N* is a key step in forming an interference estimate. As *N* increases, the resolution improves but the number of frames used to form the estimate, *L*, decreases because the signal is of finite length. A small *N* produces a well-averaged estimate but does not have enough detail to recover the frequency-hopped signal. For instance, a window size of 4,096 points lacks the resolution to accurately represent the detail in the spectrum. The resolution for the plot is

$$\Delta f_{res} = \frac{1}{NT_s} = \frac{F_s}{N} = \frac{50 \text{ MHz}}{4{,}096} \approx 12.207 \text{ kHz}, \tag{2}$$

where $N = 4{,}096$. An FFT of the received signal with only 4,096 points is shown in Figure 7 to illustrate the difficulty in using an estimate with considerable error. The FFT has the general shape of the interference signal but contains many small nulls as a result of having only 4,096 points to represent the spectrum.

Since 4,096 is a factor of the signal length, 1,032,192, the FFT window size was increased in increments of 4,096 until satisfactory resolution was achieved. Integer multiples of 4,096 ensure that the entire signal is averaged. If the window size does not divide evenly into the length of the signal, then a portion of the final samples in the signal may be excluded from the average. Thus, it is important to use an integer number of frames in the average.

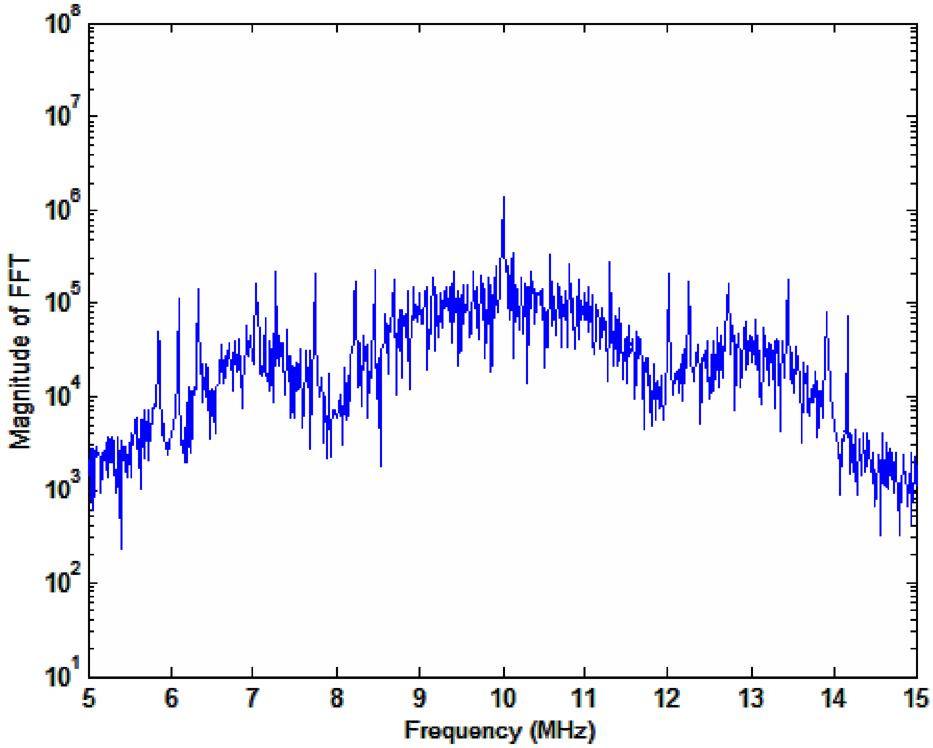

Figure 7. A 4,096-point FFT of the received signal.

The signal file is a finite length and, as a result, as the FFT window size grows, the number of FFTs that are used to calculate the average decreases. This results in an interference estimate that is formed from a small number of FFTs. Examination of window sizes from 8,192 points to 147,456 points proved that more than one FFT size is suitable to produce a detailed estimate of the interference. Any size FFT window can be used to form an estimate of the interference as long as it meets the requirements set by

$$\frac{N}{F_s} = \frac{1}{\Delta f_{res}} \leq T_{hop} \qquad (3)$$

where F_s is the sample rate, T_{hop} is the duration of a frequency hop, Δf_{res} is the resolution in the plot, and N is the FFT window size. This limit ensures that the window size N does not exceed the number of samples taken in a single frequency hop period. Averaging a smaller number of frames than there are frequency hops in the signal gives an invalid estimate by not allowing enough frames to average out the frequency hops. Moreover, computing the FFT of a large frame size can be computationally intensive and limit the speed at which an estimate can be formed. In Table 2, a list of window sizes is compared with the number of frames used to form the estimate and the approximate resolution.

FFT Window Size	**Number Of Windows Averaged**	**Approximate Resolution, Δf_{res} [Hz]**
4,096	252	12,207
8,192	126	6,104
16,384	63	3,502
24,576	42	2,035
40,960	25	1,221
81,920	12	610
147,456	7	339

Table 2. Comparison of the relative FFT size, the number of FFTs averaged together to form the estimate, and the approximate resolution.

For this thesis an FFT window size of 24,576 points was chosen. It should be noted that although this window size was not chosen arbitrarily, other window sizes would have sufficed. This frame length provided enough detail to depict frequency hops but also allowed the estimate to be calculated from 42 frames. As the number of frames used in the average increases, the frequency-hopped signal is diminished more.

To ensure this window size meets the requirements set forth in (3), further inspection is required. Each signal was sampled at 50 MHz. The sampling period then is

$$T_s = \frac{1}{F_s} = \frac{1}{50 \cdot 10^6} = 20 \text{ ns.} \tag{4}$$

From the sampling period and the frame length of 24,576 points, we can calculate the window duration with

$$(24,576 \text{ samp/s})(20 \text{ ns}) = 491.52\ \mu\text{s.} \tag{5}$$

With seven hops in the time signal and the sampling rate of 50 MHz, the length of the time signal is

$$(1,032,192 \text{ samp})(20 \text{ ns/samp}) = 20.64384 \text{ ms.} \tag{6}$$

The duration of a hop is then

$$20.64384 \text{ ms}/7 = 2.94912 \text{ ms/hop}, \tag{7}$$

making the hop rate

$$1/2.94912 \cdot 10^{-3} \text{ s} \approx 339 \text{ hops/s.} \tag{8}$$

From (5) and (7), a window size of 24,576 points is well under the limit set in (3) since

$$491.52\ \mu\text{s} \leq 2.94912\ \text{ms}. \qquad (9)$$

With a FFT size selected, the weight factor variable in the exponential average, R, can be selected.

C. WEIGHT DETERMINATION

The weight factor is the most important attribute of the exponential averaging algorithm. There is less flexibility in choosing a weight than in deciding on an FFT window size. A change in the weight factor, as little as 0.05, can provide noticeably different results. From (1), it can be seen that the weight factor is the parameter that emphasizes a particular frame, thus regulating the contribution a single frame has on the overall estimate. A small weight factor accentuates the early-time hops in the sequence because each new frame only contributes a small amount to the estimate; hence, the effect of the early-time hops does not rapidly diminish. As a consequence of a small weight, a frame containing a frequency hop receives a large immediate reduction in power when multiplied by R, but the residual power decays more slowly than when a larger weight is used. A large weight factor emphasizes the late-time hops, causing their immediate contribution to the estimate to be large. Although the frames containing the late-time hops are accentuated with a large weight, the residual power of the frames containing early-time hops is quickly attenuated by the factor of $1-R$. For a large R, the $1-R$ factor significantly deemphasizes the lingering frequency hop power left in the reference frame of the interference estimate. A balance must be struck between these two conditions by selecting a weight factor that allows the contributions from individual hops to be as uniform as possible.

Figures 8, 9, 10, and 11 are plots of the interference estimates for different weights. Each weight has tradeoffs between slightly degrading many of the frequency hops from the estimate and reducing hop power for all but a few hops. For instance, in Figure 8 the effects of using a weight factor of 0.05 to form the estimate can be seen. This weight creates an estimate with a nice shape of the interference spectrum but does not average out a single frequency hop. All seven hops can be seen in the estimate, and those at 12.07 MHz and 6.9 MHz still have significant amounts of power. Although the hop power is noticeably reduced, this weight is not successful in removing the frequency-hopped signal from the spectrum. With significant portions of the desired signal remaining in the estimate, there is a risk that none of the hops will be recovered.

A weight factor of 0.15 was used to form the estimate shown in Figure 9. This estimate has more encouraging results than an estimate using a weight of 0.05. The contribution of the frequency hop at 9.58 MHz is more significant because it is the last hop in the sequence and thus weighted by *R* the fewest number of times. The tradeoff for having a large hop at 9.58 MHZ in the estimate is a greater reduction in the power of other frequency hops. The hop at 12.07 MHz is large in this estimate, but little can be done to reduce that hop without severely impacting others because it is in the middle of a spectral null.

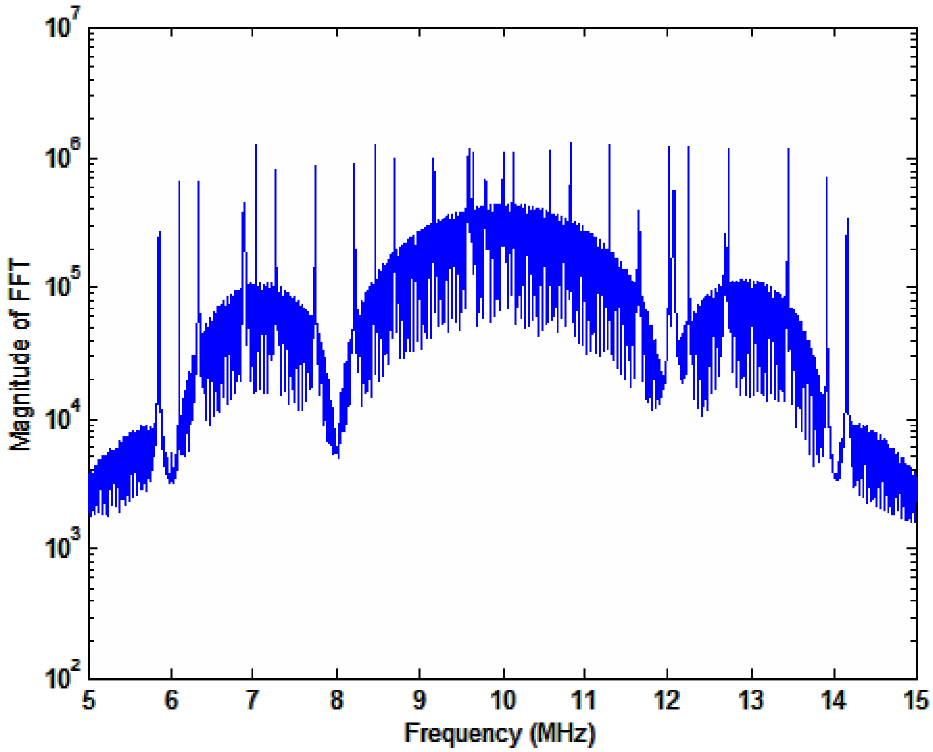

Figure 8. Interference estimate formed from weight of 0.05.

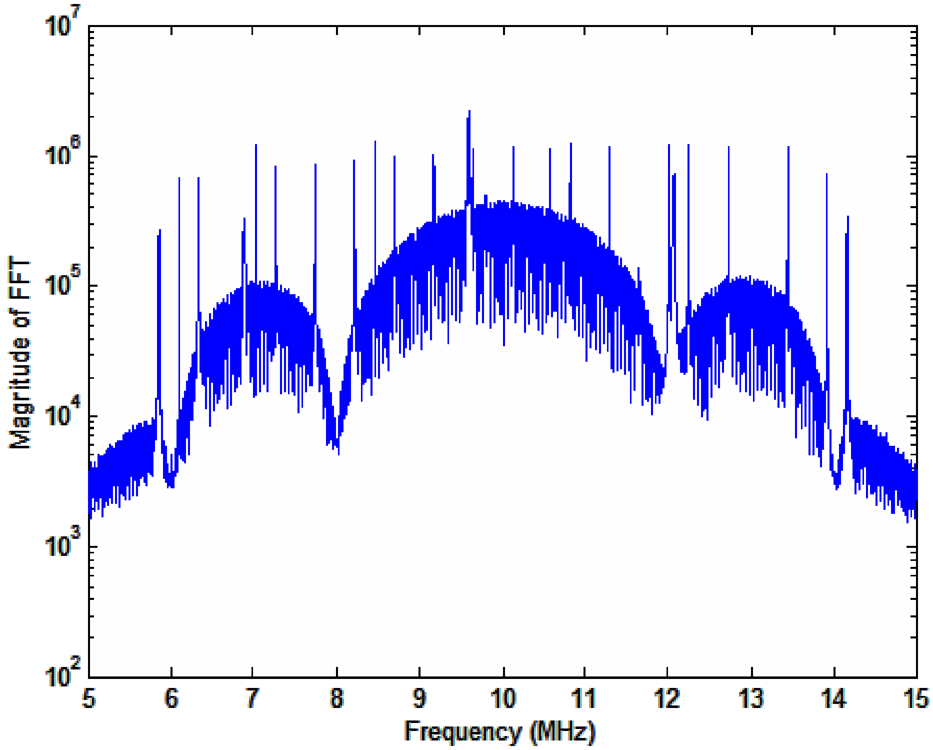

Figure 9. Interference estimate formed from weight of 0.15.

A weight factor of 0.25 provides results similar to that of a weight of 0.15. The last hop in the sequence has a larger power in the estimate, but the frequency hop at 6.9 MHz is reduced below the power level of the BPSK signal. A plot of the power spectral density of the estimate is shown in Figure 10.

A plot of the estimate using a weight of 0.5 is shown in Figure 11. This weight is not a good number to use in the exponential average. It forms half of the estimate from the last frame and the other half of the estimate from the previous 83 frames. This is undesirable because the final hop at 9.58 MHz has approximately 10 dB more power than the BPSK signal at that frequency, making it a considerable part of the interference estimate. When the interference estimate is used to recover the frequency-hopped signal, the last hop will be treated as interference and will not be recovered. Furthermore, the estimate provides a rougher estimate of the BPSK spectrum than estimates obtained with a smaller weight. The variation in the shape of the BPSK spectrum is greater, resulting in an estimate that is not as smooth as the estimates obtained with smaller weights. This deviation could provide problems when this estimate is used to resolve the frequency-hopped signal. Although the estimate is not perfect, a reduction in the power of the frequency hops to as close as possible to the peak power spectral density of the BPSK signal is desired. A weight of 0.5 reduces five hops to that level but is unsatisfactory because the estimate places too much emphasis on the last hop and the shape of the BPSK spectrum is noticeably coarse.

In Table 3, a list of weights and the respective number of hops left in an estimate formed with that weight is shown. Smaller weights leave the most frequency hops in the estimate, and the number decreases as the weight grows larger. The table leaves out the qualitative effects of each weight factor though, not showing that, as weights increase, the powers of the remaining hops in the estimate increase. The hops left after using a weight of 0.5 have a large amount of power in the estimate, and the powers of residual hops only grow when larger weights, such as 0.7, are used.

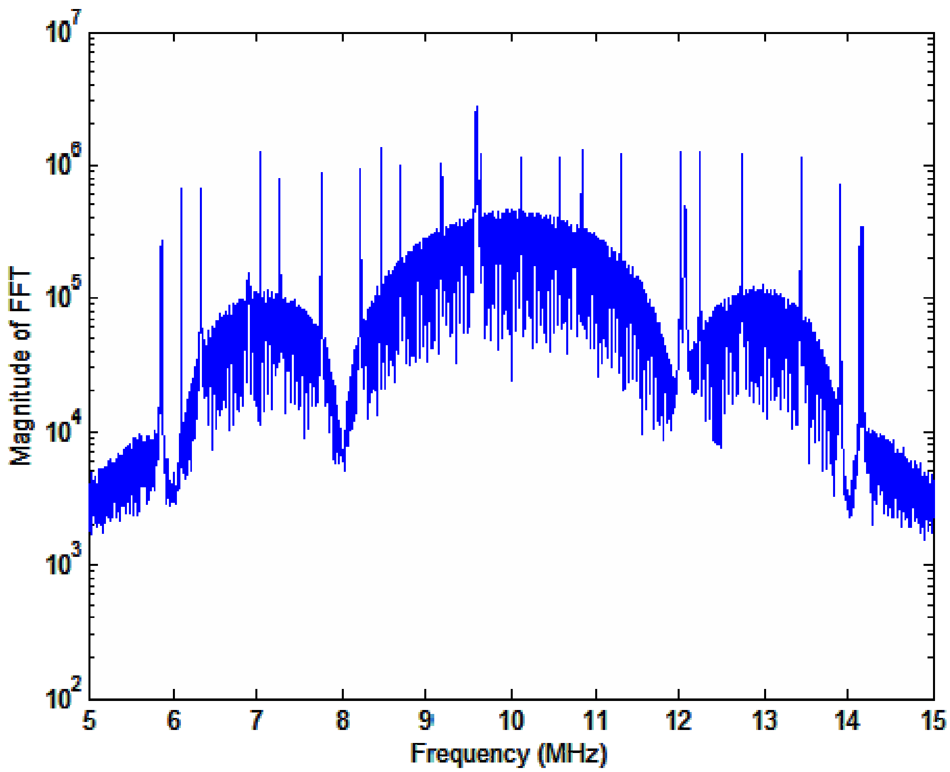

Figure 10. Interference estimate formed from weight of 0.25.

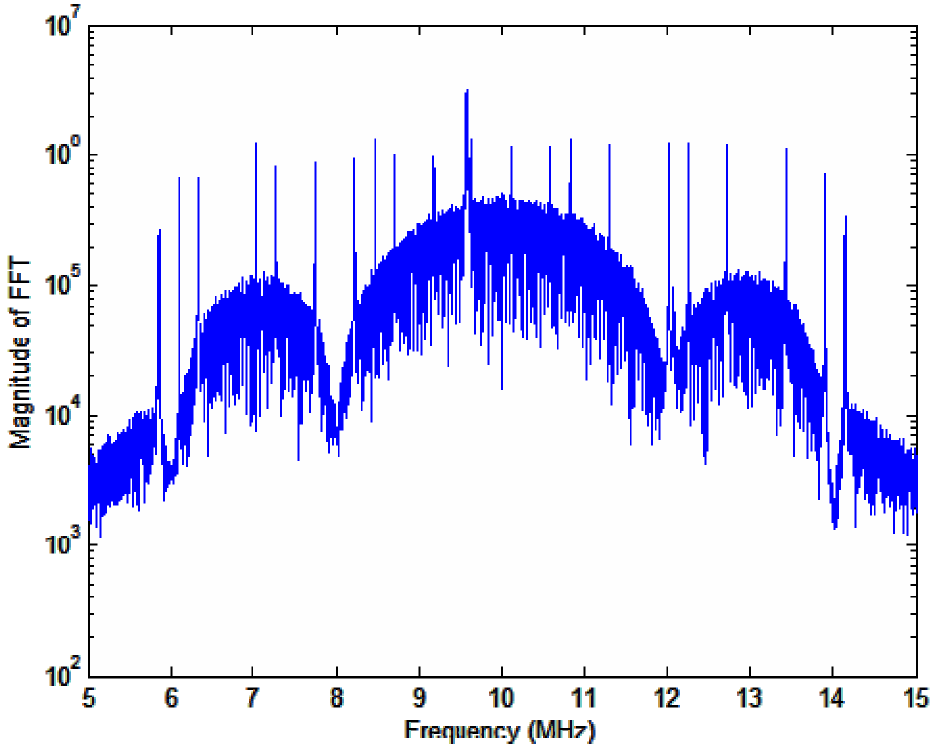

Figure 11. Interference estimate formed from weight of 0.5.

Weight	Number Of Hops Remaining
0.01	4
0.05	7
0.1	4
0.15	3
0.2	3
0.25	2
0.3	2
0.4	2
0.5	2
0.7	1

Table 3. Number of frequency hops remaining in interference estimate for given weight.

From the plots of the interference estimates, a weight between 0.15 and 0.25 was determined to be the ideal factor to use in the exponential average algorithm. Weights in this range stress individual frames as equally as can be expected for an algorithm that does not know the duration of the signal at the start of executing the algorithm. To determine the best weight factor for recovering the frequency-hopped signal, the different estimates must be tested to determine which estimate recovers the most frequency hops.

In this chapter, the development of a frequency-domain estimate of an interference signal eclipsing a desired frequency-hopped signal was discussed. With an exponential average of FFT windows, a frequency-hopped signal can be removed quite well from the estimate. With a weight factor of 0.25 and a window size of 24,576 points, an accurate estimate of the interference signal spectrum was obtained. In the next chapter, we examine various methods that utilize the interference estimate for detecting the frequency-hopped signal embedded in the interference.

IV. FREQUENCY HOP RECOVERY

With acceptable estimates of the interference signals, a method was developed for resolving the frequency-hopped signal buried within the noise. Two approaches were examined: spectral subtraction and spectral division. The goal of the two techniques is to exploit the difference between the interference estimate and the received signal. Ideally, that difference should be only the desired frequency-hopped signal. Since real signals are not easy to estimate, the objective was to find the best case from either of the two methods. In order to accomplish the mathematical calculations of array values, the power spectral density of the received signal had to be the same length as the estimate. Once the estimate was formed, a frame-by-frame calculation was made. The results were then summed to create a final spectral picture that was 24,576 points long.

A. SPECTRAL SUBTRACTION

Spectral subtraction assumes that the frequency-hopped signal has more power than the interference signal at each of the hop frequencies. The subtraction algorithm operates on the principle that a hop with 1-2 dB more power would be recognizable once the interference was removed. Spectral subtraction, however, turned out to be an unsuccessful method for recovering frequency hops.

Since the estimate is imperfect, it is not able to calculate the actual power levels at each frequency; only the general shape of the spectrum is preserved with the exponential average. As a result, spectral subtraction highlights the difference between assumed and actual power levels of the interference signal. The result, known as the difference spectrum, then retains the same general shape as the interference signal. No separation between the frequency-hopped signal and the interference signal was obtained, and the FH/MSK signal remained embedded in the interference signal. In Figure 12 a plot of the difference spectrum is shown. It is noteworthy that at 9.58 MHz and 12.07 MHz hops are recognizable but all other hops could easily be confused with noise and cannot be accurately resolved.

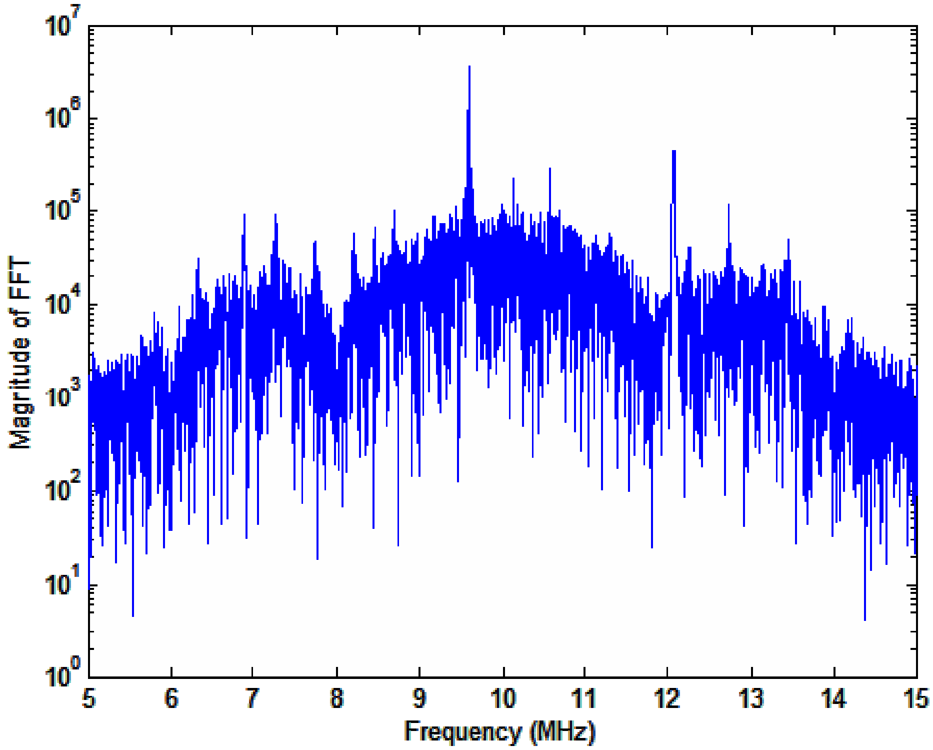

Figure 12. Power spectral density of spectral subtraction signal, weight factor $R = 0.25$.

The failure of spectral subtraction to resolve the frequency-hopped signal highlights the fact that numerical power levels in the estimate are not the important factor. The comparative shape between the estimate and the received signal are the keys to detecting the frequency-hopped signal. Normalization through division exploits the shape of the estimate rather than comparing the power levels in the two spectrums.

B. SPECTRAL DIVISION

As a byproduct of the spectral subtraction results, the idea of division was developed. If the frequency-hopped signal can viewed relative to a noise floor and not the interference signal as with the original composite received signal, then the power difference at the hop frequencies should be noticeable.

A frame-by-frame division of the received signal by the estimate was computed. Again the results were summed, and a 24,576-point power spectral density showed the difference in shape of the received signal and the estimate rather than the difference in power. The frequency-hopped signal had then been normalized against the interference signal and was able to be viewed as if it were the only signal in the band when received. A type of receiver that implements division of the received signal with the noise power is known as a noise-normalized receiver. Considerable analysis has been done in the past on these types of receivers, and the calculated theoretical performance asserts that noise-normalized receivers significantly reduce bit error rates. Previous work on noise-normalized receivers in [6], [7], [8], and [9] assumes that the received noise is uniform and Gaussian, a considerably different case compared to the interference signals considered in this thesis. None of these references discusses implementation of the receiver in hardware or simulation; all analysis is theoretical. The estimate used for normalization in this thesis is formed over the length of the signal, while in [7] and [9] the noise estimate is formed from interference present only during the hop period. With the estimate described in Chapter 3, a receiver is able to normalize the desired signal even with non-uniform noise power.

The results of the spectral division algorithm were considerably better than those achieved with subtraction. Figure 13 shows the normalized spectrum. From this spectral picture it is quite evident that frequency hops are present in the received signal. Although not all the hops are present, division with the estimate yields a majority of the frequency hops. Using a weight of 0.25, five of the seven transmitted frequency hops are clearly defined in the spectrum. The two missing hops are the sixth and seventh in the sequence. The hops are numbered with the order in which they were transmitted. Hop 6 is buried in the noise floor and hop 7 appears to be negative relative to the noise floor.

The estimate formed with a weight factor of 0.l5 was also used to normalize the received signal. The smaller weight did not yield as many frequency hops as the estimate that used 0.25. Hops 6 and 7 are unable to be recovered, but the fifth hop in the sequence is too close to the noise floor to be resolved as well. In Figure 14 the normalized spectrum is shown after 0.15 was used for the estimate weight factor. The noise floor in that spectrum has less power than the floor in Figure 13 for a weight of 0.25. Although this is an attractive quality, 0.25 still allows the recovery of the most frequency hops.

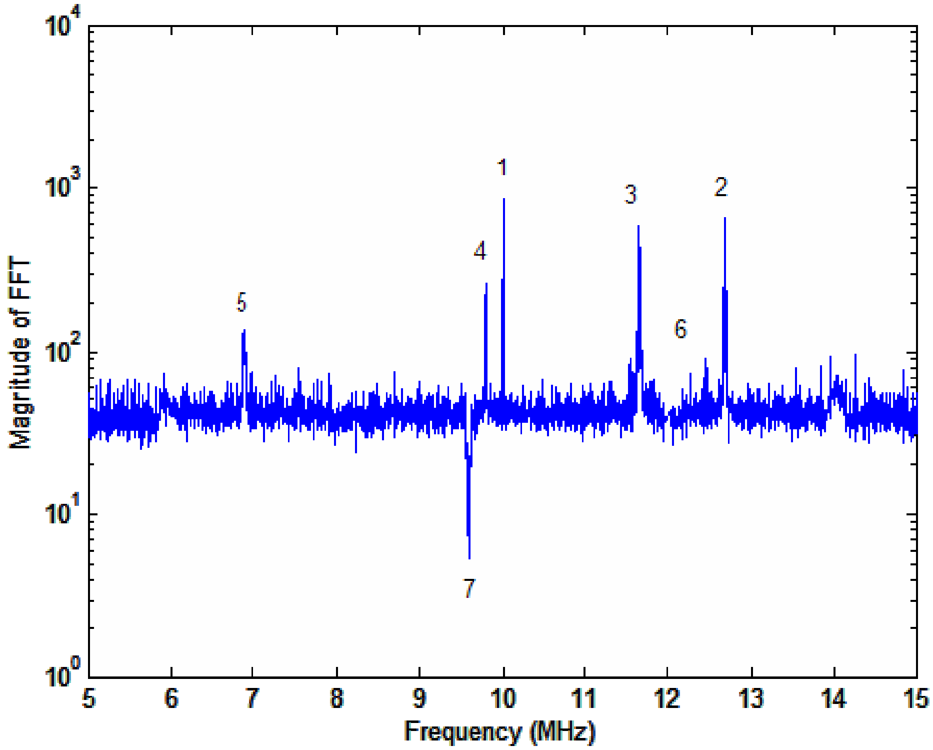

Figure 13. A plot of the power spectral density of the normalized spectrum, $R = 0.25$.

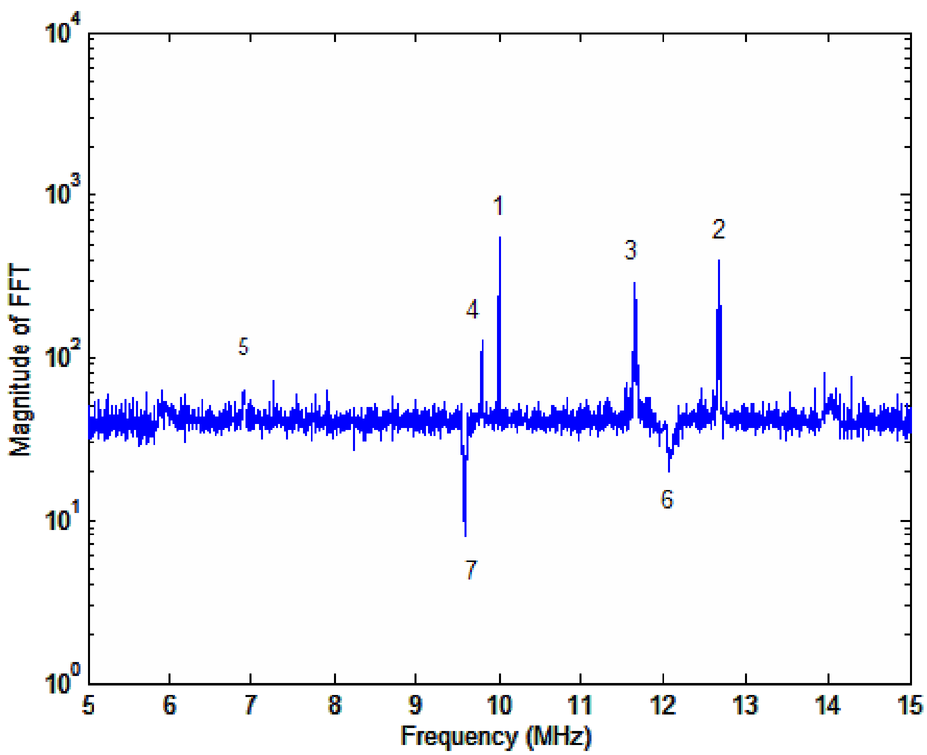

Figure 14. A plot of the power spectral density of the normalized spectrum, $R = 0.15$.

In order to confirm that estimates formed using other weight factors would not perform as well as a weight of 0.25, other weights such as 0.5 and 0.05 were tested. As expected, these weights did not provide an estimate accurate enough to recover the frequency-hopped signal as well as a weight of 0.25. In Figure 15 a plot with the normalized spectrum for $R = 0.05$ is shown. Although the spectrum is very clean, only four hops were recovered.

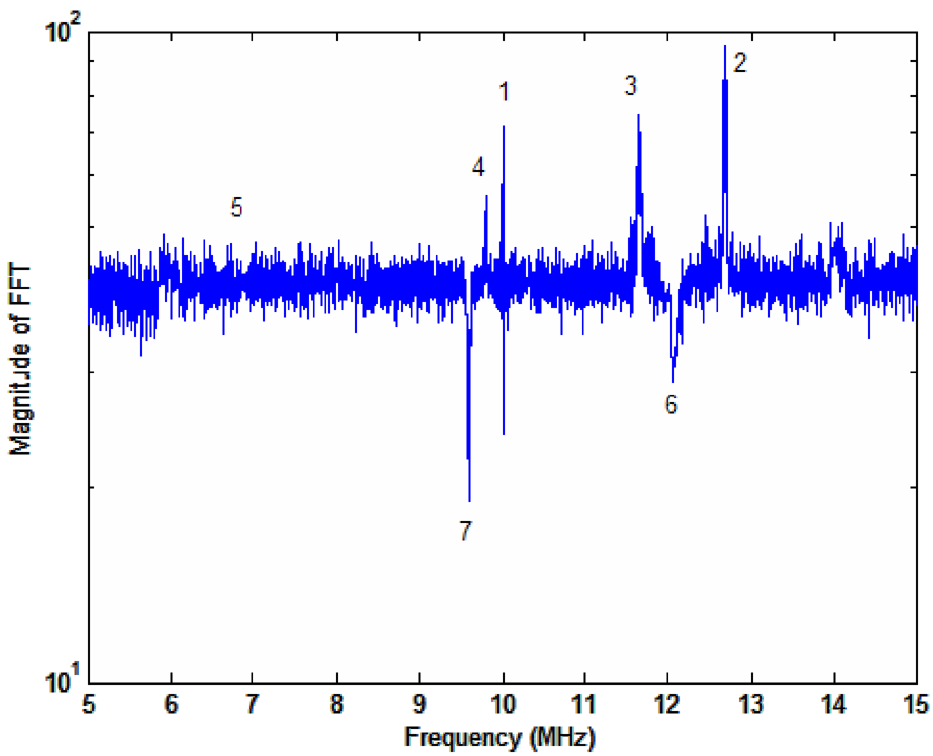

Figure 15. A plot of the power spectral density of the normalized spectrum, $R = 0.05$.

Increasing the weight does not cause more frequency hops to be recovered either. As shown in Figure 16, with a weight of 0.5, six hops can be seen but are difficult to distinguish from the noise floor in the spectrum. Both hops five and six could be mistaken for noise spikes, and it would be difficult to recover the demodulated signal amidst the higher noise levels. As the weight factor increases, the noise variance relative to the frequency-hopped signal increases and eventually overcomes the reduction in noise power provided by normalization. A weight factor of 0.5, as well as larger weights, caused the noise variance to increase because much of the estimate is formed from the last window in the received signal. With so much emphasis placed on the last frame, the estimate is less of an average and instead relies on the final window being similar to every other window in the received signal. It is not, however, and much of the noise arises because the average has not been able to smooth out the shape of the estimate.

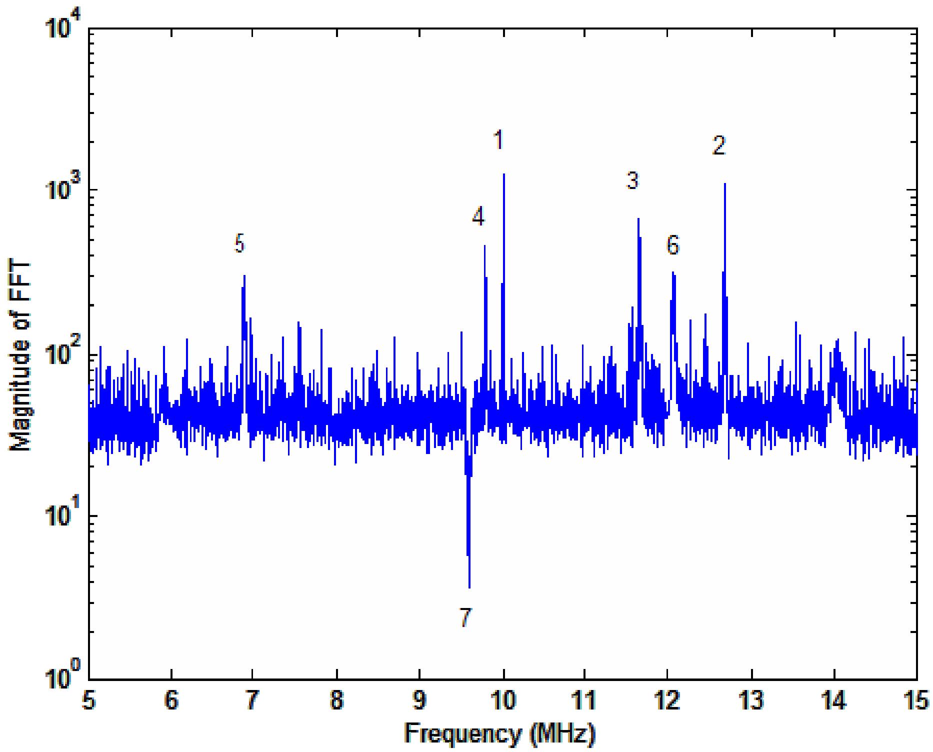

Figure 16. A plot of the power spectral density of the normalized spectrum, $R = 0.5$.

From the previous figures, it is evident that a weight of 0.25 resolves the most frequency hops without exciting the noise floor too much. This makes recovery and demodulation of a frequency-hopped signal an easier task. Using this weight, we assumed that all but the last two frequency hops transmitted could be recovered using the noise-normalization technique described. In order to determine how this technique performs with longer received signals, a transmitted signal was used that had a noise file appended after the transmission of the frequency-hopped signal had ended. This is discussed in the next section.

C. NOISE-NORMALIZATION WITH EXTENDED RECEIVED SIGNAL

Under the theory that forming the estimate from a longer signal contributes to the detection of late-time frequency hops, a simulation was run to determine if all seven frequency hops in the signal could be recovered. A noise file was appended to the end of the received signal to give the estimate more time to normalize the received signal.

1. Extended Signal with Appended Noise

A received signal file was formed from the original received signal from Chapter II, and then a 1,032,192-point file containing only the interference waveforms was appended at the end. This file was then twice the size of the original received signal. This signal simulates a frequency-hopped waveform being received amidst interference waveforms but, when transmission of the frequency-hopped signal stops, the receiver still continues to receive the interference waveforms. A spectrum of this signal looks the same as the spectrum shown in Figure 4. The time signal is different, however, than the original received signal. A plot of the received signal in the time domain is shown in Figure 17.

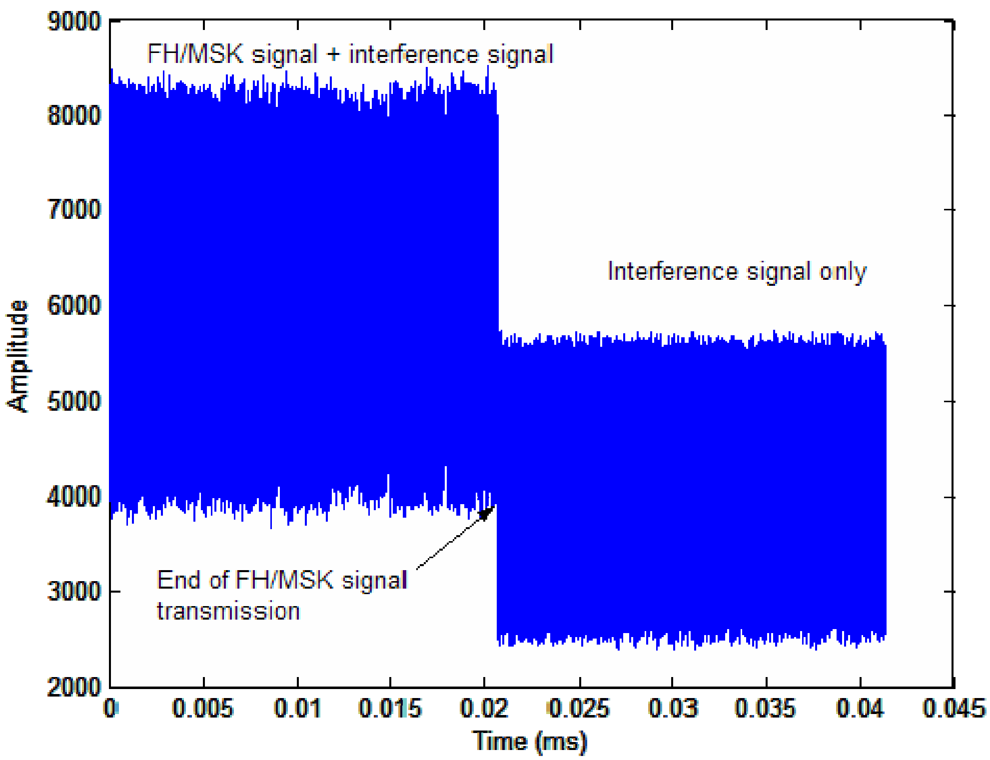

Figure 17. Time domain plot of extended received signal.

2. Simulation results of extended received signal

After normalization, the spectrum of the extended received signal (Figure 18) looked very clean. All seven frequency hops are clearly shown. From this simulation, it is evident that, as a discrete signal grows in length and L increases, frequency hops received in the i-th window of the signal, where i is small compared to L, can be resolved with more clarity.

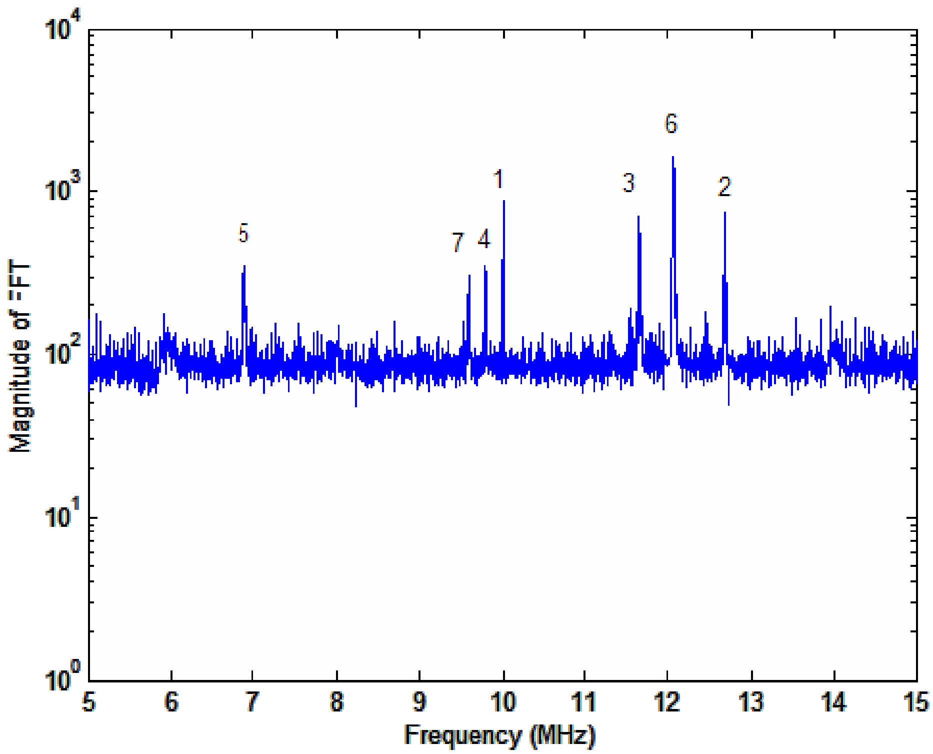

Figure 18. Plot of power spectral density of extended received signal after normalization.

As a result of the increase in L, the contribution from earlier windows is reduced in the estimate. The window that contains the seventh hop in the sequence is no longer the last frame, and thus no longer a large portion of the estimate. This was the reason the seventh hop could not be resolved in previous simulations. A window that encompasses the last frequency hop, the 42^{nd} of 42 windows, is now the 42^{nd} of 84 windows. The 42^{nd} window had previously been multiplied by $R = 0.25$. The weight factor on that individual frame is now

$$\left(R\right)\left(1-R\right)^{\left(L-i\right)}=\left(0.25\right)\left(0.75\right)^{\left(84-42\right)}\approx 1.4\cdot 10^{-6}. \quad (10)$$

The contribution of the 42^{nd} frame to the interference estimate is virtually zero, thus creating an estimate with no frequency hop components. From these results, it is clear that the algorithm should be able to resolve the first $k-2$ hops in a k hop signal. This is examined in the next section.

D. NOISE-NORMALIZATION WITH EXTENDED TRANSMITTED SIGNAL CONTAINING FOURTEEN FREQUENCY HOPS

Although noise-normalization was able to resolve most of the frequency hops in the received signal, another simulation was devised to test if $k-2$ hops in a k-hop signal could be detected. A signal with fourteen frequency hops was created for this simulation.

1. Signal with Fourteen Frequency Hops

Since no signal with a greater number of frequency hops was available, a file was created using the original frequency-hopped signal. The seven hops were shifted in frequency to new, unique carriers and concatenated in time with the original FH/MSK signal to provide a signal with $k=14$ frequency hops. To achieve this, a frequency shift was applied to create seven new hop frequencies. Using the Fourier transform property [10]

$$e^{j2\pi f_0 t} \overset{F}{\Leftrightarrow} \delta\left(f-f_0\right) \quad (11)$$

to shift the frequencies, the time domain signal was multiplied by $e^{j2\pi f_0 t}$, where $f_0 = 1.3$ MHz. A frequency-domain plot comparing the original seven hops and the seven shifted hops is shown in Figure 19.

The spectrum of the complete fourteen-hop signal is shown in Figure 20. The hop sequence for the signal is shown in Table 4. Because the fourteen-hop signal was comprised of two concatenated signals, the first seven frequency hops are the same as the original signal and the last seven hops are transmitted in the same sequence as the first seven. The concatenated signal is 2,064,384 points long.

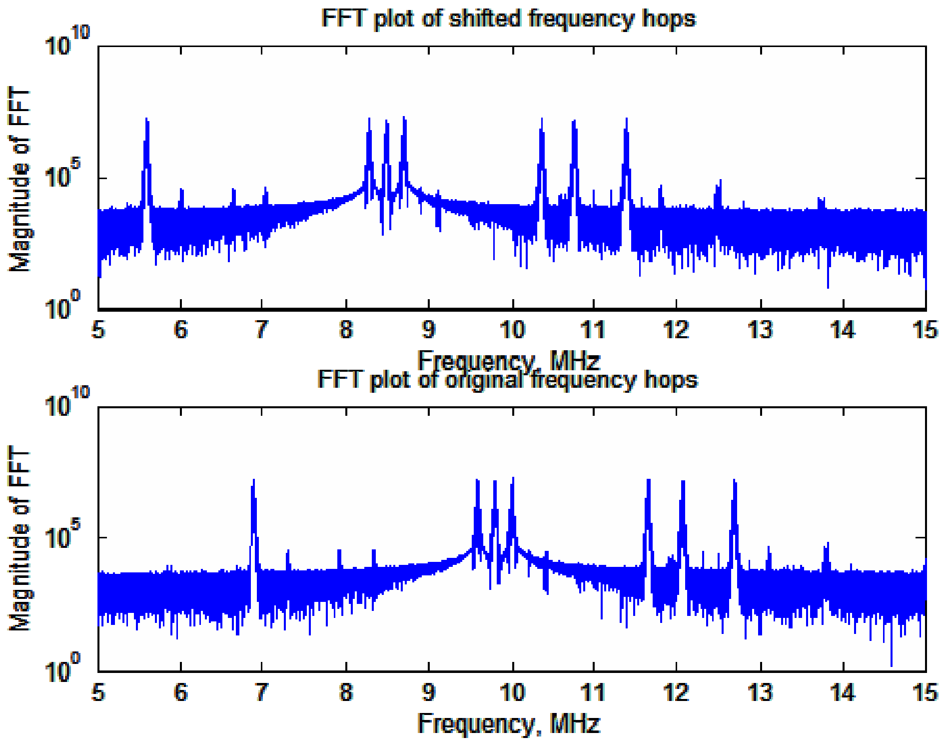

Figure 19. Plots comparing spectrums of original and shifted frequency-hopped signals.

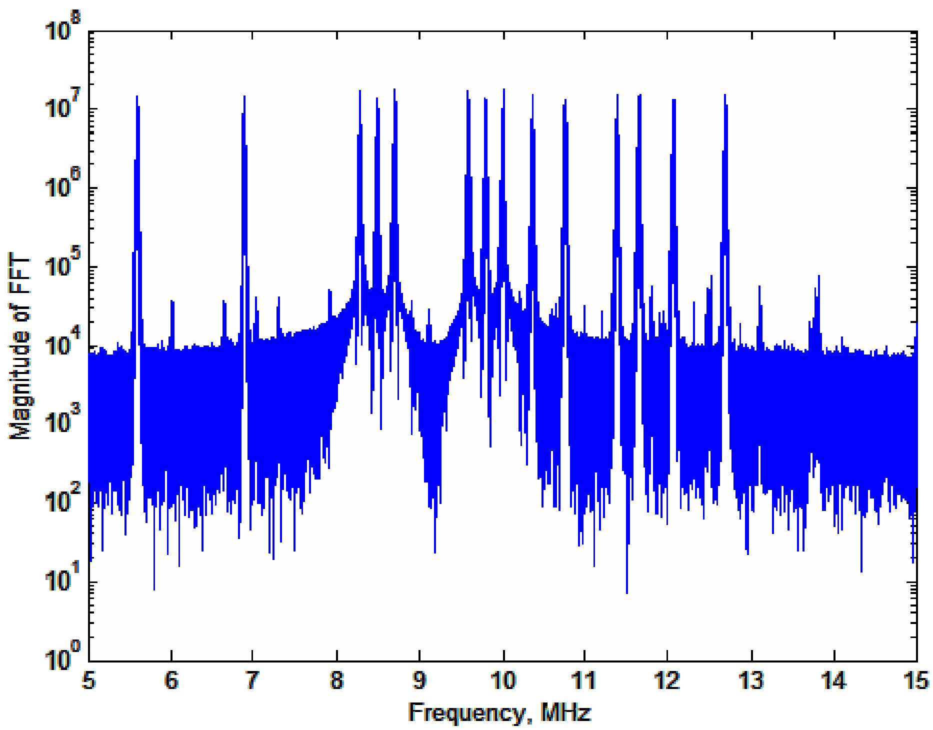

Figure 20. Power spectral density of frequency-hopped signal with fourteen hops.

Carrier Frequency [MHz]	Hop Number
5.6	12
6.9	5
8.28	14
8.5	11
8.7	8
9.58	7
9.8	4
10	1
10.35	10
10.78	13
11.39	9
11.65	3
12.07	6
12.7	2

Table 4. Frequencies and sequence order of hops in extended, 14-hop FH/MSK signal.

2. Extended Signal Detection Results

As the weight increases, more noise is left in the normalized spectrum. Increased weight factors also place greater emphasis on later hops in the sequence, accentuating hops that would not be detected with smaller weights. A weight of 0.3, slightly larger than the weight factor of 0.25 used in Section B, provided the best normalized spectrum. Although a weight factor of 0.25 was satisfactory, the hop at 5.6 MHz was clearer when $R = 0.3$. For every seven hops transmitted, six were resolved. In this simulation twelve of the fourteen hops that were transmitted are visible in the normalized spectrum. A plot of the power spectral density of the normalized signal is shown in Figure 21.

Similar to the results discussed in Section B, small weights such as 0.05 and 0.15 do not resolve as many frequency hops as larger weight factors. Any weight factor above 0.3 in this simulation made it too difficult for certain hops to be differentiated from the noise floor.

From these results it is clear that normalization of the spectrum allows six of every seven hops to be resolved if a weight of approximately 0.25 to 0.3 is used. This upper limit of six hops per every seven is a positive result when compared to interference waveforms remaining in the received spectrum and no hops being detected. It is important to note that all of the first seven hops in the sequence were resolved. The only two hops not resolved were numbers thirteen and fourteen in the sequence. From this it can be assumed that the earlier a hop is in the sequence, the more likely that it will be resolved. This follows intuitively because only the late-time hops were not averaged out in the estimate. Since hops thirteen and fourteen are significant in the estimate, they do not stand out when the received signal is normalized by the estimate.

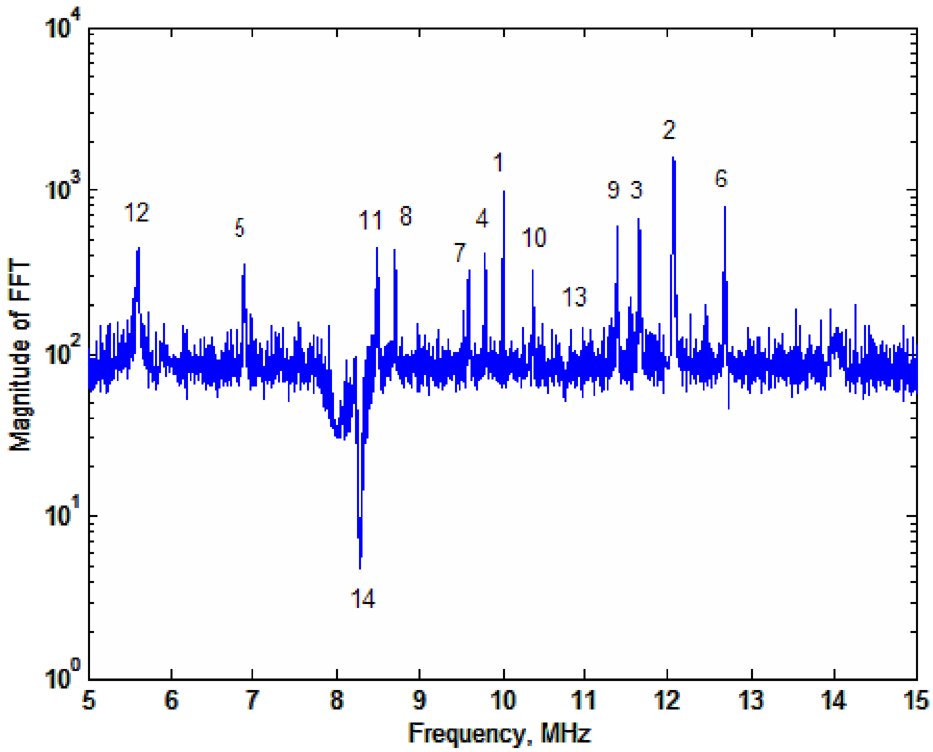

Figure 21. Normalized spectrum of extended received signal, $R = 0.3$.

In this chapter, several simulations were used to test methods for resolving a frequency-hopped signal. Subtraction of the estimate from the received signal proved to be an inadequate method for detecting the frequency-hopped signal because too much noise remained in the difference spectrum. Spectral division, or noise-normalization, however, is a technique that successfully resolved the frequency-hopped signal embedded in interference. With this technique, $k-2$ hops in a k-hop signal can be recovered. The next chapter focuses on the performance of noise-normalization with regards to the bit error rate and interference power reduction.

V. BIT ERROR RATE SIMULATION

A simulation measuring the effectiveness of the noise reduction algorithm was tested with a new transmitted signal. The goal was to determine the reduction in interference signal power necessary to achieve the same probabilities of bit error (i.e., bit error rates (BERs)) for a received signal, viewed after the channel noise had been normalized.

A. SIMULATION DESCRIPTION

Three simulations were needed in order to characterize the effects of the normalization technique. A frequency-hopped, binary frequency-shift keyed signal (FH/BFSK) was transmitted in a channel with various types of noise. If perfect de-hopping is assumed at the receiver, then the received signal is a BFSK signal embedded in interference. To test this, additive white Gaussian noise (AWGN) was added to the channel as well. The first simulation measured the BER for a MATLAB-generated BFSK signal in AWGN. Figure 22 shows a block diagram of the simulation. The second simulation was of the BFSK signal transmitted through a channel that contained BPSK and CW waveforms as well as AWGN. The same BPSK and CW waveforms described in Chapter II were used for the simulation. The block diagram shown in Figure 23 describes this simulation. The third simulation measured the BER for a BFSK signal transmitted over a channel with AWGN and a normalized interference signal. This interference signal was created by computing the inverse fast Fourier transform (IFFT) of a normalized composite BSPK and CW interference signal. This signal is known as the normalized interference signal. A block diagram describing the simulation is shown in Figure 24. In this simulation the performance of a communications signal sent through a channel with normalized interference power levels is examined. With a normalized interference signal, noise power levels should be significantly lower than the simulation shown in Figure 23. The reduction in interference power was measured by comparing the bit error rates from the simulations before normalization and after normalization.

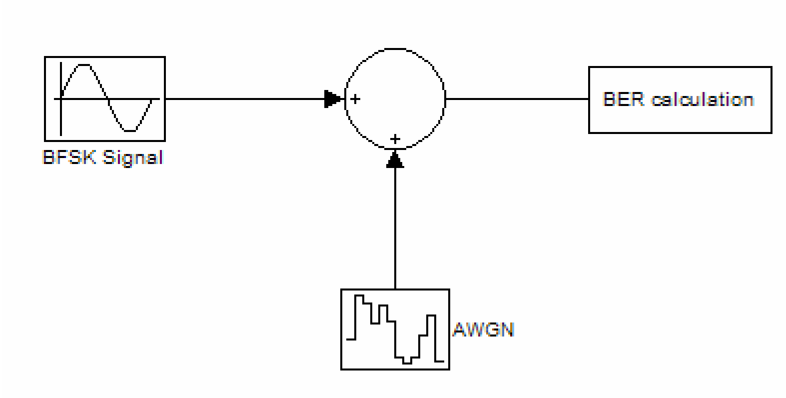

Figure 22. Block diagram of simulation measuring bit error rate for received signal in channel with AWGN.

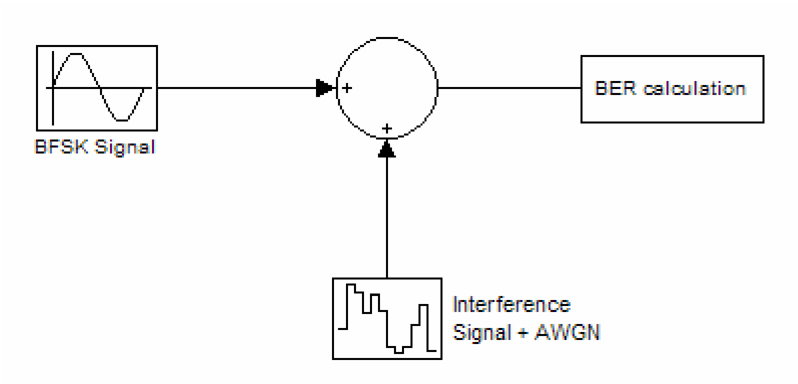

Figure 23. Block diagram of simulation measuring bit error rate for received signal in channel with AWGN and interference signal.

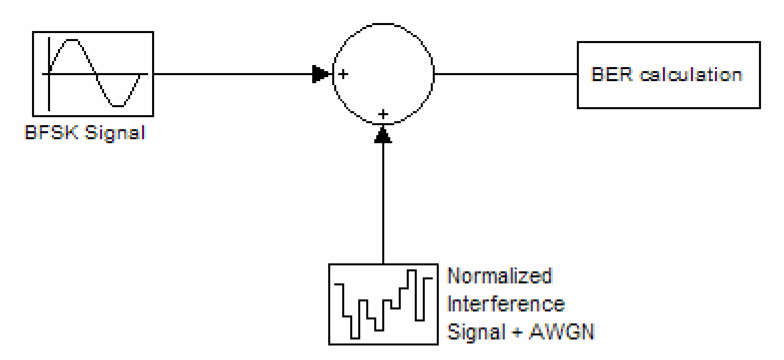

Figure 24. Block diagram of simulation measuring bit error rate for received signal in channel with AWGN and normalized interference signal.

B. SIMULATION RESULTS

The signal transmitted through a channel with just AWGN was received with an approximate probability of bit error of 0.001. To determine the BER for the 65,536 transmitted bits, a BFSK-receiver simulation, standard as part of the MATLAB communications toolbox, mapped the received symbols to bits and compared each with the transmitted bits. With interference waveforms present in the channel, the BER degraded to approximately 0.44. This level of bit error rate is essentially receiver failure because the receiver is forced to guess, correctly choosing the transmitted symbol only half of the time.

The probability of bit error for the channel with a normalized interference signal and AWGN was 0.001. Since this is the same as with only AWGN, the capabilities of the normalization scheme are best characterized by the amount that the algorithm reduces the power of the interference signal. In order to quantify this reduction, the power of the transmitted interference waveforms was reduced until the same bit error rate as the simulation with a normalized interference signal was achieved. The plot in Figure 25 shows how the bit error rate changed with a reduction in interference signal power. As seen in Figure 25, the bit error rate drops dramatically as the interference signal power is reduced. In order to achieve the same bit error rates in the simulation as with normalized interference and AWGN, the interference signal power had to be reduced by 50 dB. It can be assumed that the noise-normalization technique could achieve the same reduction in interference signal power when used for a real-time reception.

This bit error rate simulation provides a quantitative characterization of the noise-normalization effects. Use of the normalization technique yields bit error rates equal to those of a 50-dB reduction in interference signal power. From this, it can be assumed that noise-normalization reduces interference by 50 dB in the frequency-hopped band. Chapter VI uses this result to draw conclusions about the detection of frequency-hopped signals embedded in interference waveforms.

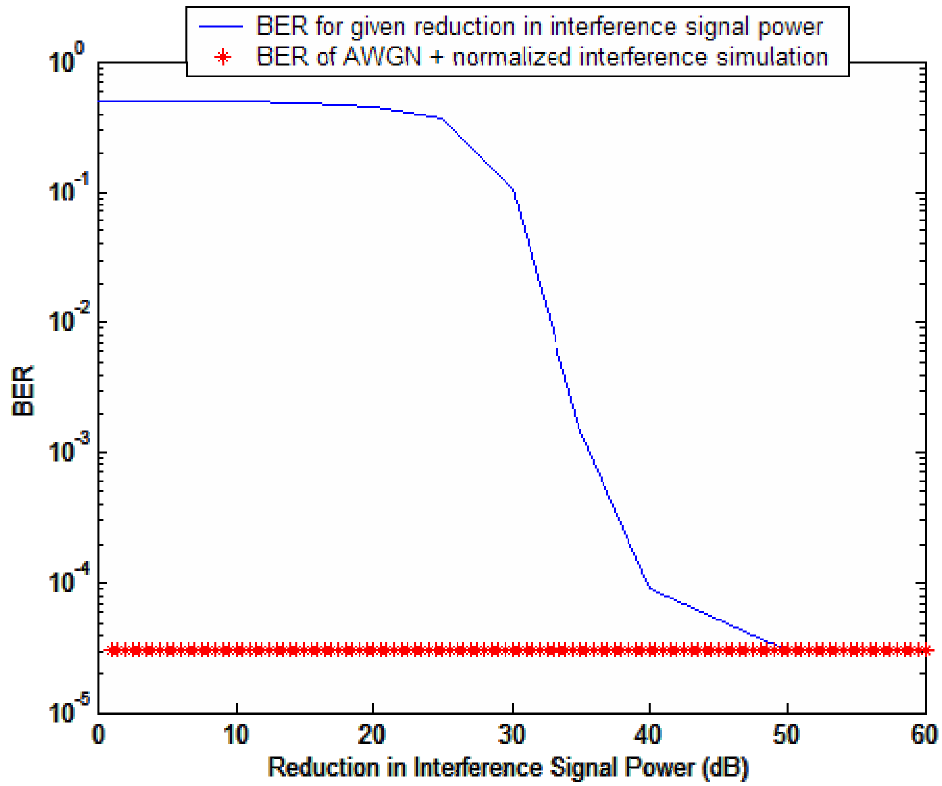

Figure 25. Plot of reduction in interference signal power vs. bit error rate along with plot of BER for simulation with noise signal containing AWGN and normalized interference signals.

VI. CONCLUSIONS

A. CONCLUSIONS

In this thesis a technique for resolving a frequency-hopped signal embedded in interference waveforms was described. The algorithm involves creating an estimate of the interference spectrum by using an exponential average of FFT windows to create an approximate spectral picture of the interference waveforms. The variables involved in averaging the windows include the FFT size, the weight applied to each frame, and the number of frames used in the estimate. For a 24,576-point window, a weight between 0.15 and 0.25 was determined to produce the best estimate of the interference spectrum. Two methods for resolving the frequency-hopped signal were explored as well. Division of the received signal by the estimate in the frequency domain presents a cleaner power spectral density of the frequency-hopped signal than does spectral subtraction. For a weight of 0.25, five of the seven frequency hops in the desired signal were detected after normalization of the received signal. Through other simulations, it was determined that $k-2$ frequency hops of a k-hop signal can be resolved using this noise-normalization technique. Through bit error rate simulations, the normalization technique was determined to have reduced the interference waveform power by 50 dB, having achieved the same bit error rates as a 50-dB reduction in noise power.

This technique may be useful for systems implementing frequency-hopped communications such as military radios and networks as well as commercial frequency-hopped systems such as Bluetooth [11]. Although these systems do not always operate in environments that contain other waveforms which would act as jamming signals, the possibility exists that they might.

B. FUTURE WORK

The technique presented has future research potential and should be explored on a deeper level. While the method was developed for CW and BPSK-modulated interference signals, other types of waveforms that might interfere with frequency-hopped communications should be explored. These interference signals include M-ary phase-shift keying (M-PSK), M-ary frequency-shift keying (M-FSK), quadrature amplitude modulation (QAM), and orthogonal frequency-division multiplexing (OFDM). Testing in different operational environments may allow for more uses of normalization.

Furthermore, implementation of the technique in a real-time environment using simulations or hardware is another area to explore. Such an implementation would make the technique more applicable to real-time communications systems. Actual demodulation and recovery of encoded messages, as well as performance evaluations in fading channels, are steps that could be taken in future work.

More can be explored regarding the capabilities of noise-normalization by investigating the correlation between FFT window size and weight factor and the quality of normalized signal each combination produces.

LIST OF REFERENCES

[1] R. M. Dillard and G. M. Dillard, "Likelihood-ratio detection of frequency-hopped signals," *IEEE Trans. Aerospace Electronic Systems*, vol. 32, no. 2, pp. 543-553, Apr. 1996.

[2] N. C. Beaulieu, W. L. Hopkins, and P. J. McLane, "Interception of frequency-hopped spread-spectrum signals," *IEEE Journ. Selected Areas Communications*, vol. 8, no. 5, pp. 853-870, Jun. 1990.

[3] C. C. Ko, W. Zhi, and F. Chin, "ML-based frequency estimation and synchronization of frequency hopping signals," *IEEE Trans. Signal Processing*, vol. 53, no. 2, pp. 403-410, Feb. 2005.

[4] L. W. Nemsick and E. Geraniotis, "Adaptive multichannel detection of frequency-hopping signals," *IEEE Trans. Communications*, vol. 40, no. 9, pp. 1502-1511, Sep. 1992.

[5] J. G. Proakis, *Digital Communications*, McGraw-Hill, New York, 2001.

[6] M. Kragh and R. C. Robertson, "The effect of Rician fading and partial-band interference on noise-normalized, fast frequency-hopped M-FSK receivers," *Proc. IEEE Military Communications Conference, 1993,* vol. 1, pp. 182-186, 1993.

[7] R. C. Robertson and T. T. Ha, "Error probabilities of frequency-hopped M-FSK with noise-normalization combining in a fading channel with partial-band interference," *IEEE Trans. Communications*, vol. 40, no. 2, pp. 404-412, Feb. 1992.

[8] H. Iwasaki and R. C. Robertson, "Performance of a fast frequency-hopped noncoherent M-FSK receiver with non-ideal noise-normalization combining," *IEEE Military Communications Conference, 1995,* vol. 1, pp. 309-314, 1995.

[9] C. D. Chung and P. C. Huang, "Effects of fading and partial-band noise jamming on a fast FH/BFSK acquisition receiver with noise-normalization combination," *IEEE Trans. Communications*, vol. 44, no. 1, pp. 94-104, Jan. 1996.

[10] B. Sklar, *Digital Communications: Fundamentals and Applications*, 2nd ed., Prentice Hall, Upper Saddle River, NJ, 2001.

[11] M. Miller, *Discovering Bluetooth*, Sybex, Inc., Alameda, CA, 2001.

INITIAL DISTRIBUTION LIST

1. Defense Technical Information Center
   Ft. Belvoir, Virginia

2. Dudley Knox Library
   Naval Postgraduate School
   Monterey, California

3. Chair, Code EC
   Naval Postgraduate School
   Monterey, California

4. Professor R. Clark Robertson
   Naval Postgraduate School
   Monterey, California

5. Professor Frank Kragh
   Naval Postgraduate School
   Monterey, California

6. Dr. Kyle Kowalske
   Department of Defense
   Columbia, Maryland

7. Nathan Beltz
   Naval Postgraduate School
   Monterey, California

8. Ensign Christopher Brown
   USS HOWARD
   San Diego, California